

## Allosteric Modulation Of Aurka Kinase Activity By Arkin-A Via Dynamic Correlation Network Analysis

Muhammad Shahab<sup>1</sup>, Mehran Ullah<sup>\*2</sup>, Haider Ali Khan<sup>3,4</sup>, Mehreen Ghufuran<sup>5</sup>, Mohtasim Billah<sup>5</sup>, Muhammad Siddiq<sup>6</sup>

<sup>1</sup>State key laboratories of chemical Resources Engineering Beijing University of chemical technology, Beijing 100029, china.

<sup>2</sup>Medical Teaching Institution Mardan Medical Complex Mardan, Mardan 23200, Pakistan.

<sup>3</sup>Department of Health, THQ Takht Bhai, Mardan, KP - Pakistan

<sup>4</sup>Department of Biochemistry, Abdul Wali Khan University Mardan, KP - Pakistan

<sup>5</sup>Department of Pathology, Medical Teaching Institution Bacha Khan Medical College Mardan, KP - Pakistan.

<sup>6</sup>Department of Pharmacy, Abdul Wali Khan University Mardan, KP - Pakistan

### ABSTRACT

Protein phosphorylation and post-translational modification by protein kinases are crucial cell signaling and regulatory systems. Aurka, a serine/threonine kinase, controls mitotic cell division and has sequence homology with other kinases. Clinical trials are underway to target Aurka Kinase's overexpression in human cancer using ATP-competitive drugs. AurkinA, a small allosteric inhibitor, binds to TPX2's Y-pocket, which holds Y8 and Y10. AurkinA drug-like inhibitors delocalize the kinase from cell spindle formation, disrupting the Aurka-Tpx2 complex. The allosteric mechanism for these compounds is unclear at the molecular level. To understand the allosteric mechanism, all-atom molecular dynamics simulations were employed to create fluctuation association networks. The fluctuation correlation networks of Aurka-Tpx2 and AurkinA vary significantly. Aurka-AurkinA transfers information from the allosteric to the catalytic sites more readily than Aurka-Tpx2. These methods will help develop route-targeted drugs and create protein allosteric circuits.

**Study Design:** Molecular dynamics simulations, an investigative strategy, and Aurka kinase allostery.

**Duration And Place Of Study:** Department of Health, Medical Teaching Institution Mardan Medical Complex Mardan, from jan 2018 to jan 2019

**Keywords:** Aurka kinase, TPX2, AurkinA, MD simulation

### INTRODUCTION

Cells' most significant signaling and regulatory processes include protein phosphorylation and

post-translational changes carried out by proteins called protein kinases. The human genome encodes hundreds of protein kinases and many multi-domain polypeptides. And most of them have many proteins in them<sup>1</sup>. The purpose of the orthologous Aurka kinase enzyme, which belongs to the Serine/Threonine kinase family, is to maintain cell division progression during mitosis<sup>2,3</sup>. In humans, cancer is caused by overexpression of Aurka Kinase<sup>4</sup>.

The primary functions of the Aurka kinase include spindle assembly, spindle microtubule formation, centrosomal maturation, mitotic checkpoint regulation, and spindle bipolarity maintenance<sup>5</sup>. Numerous binding partners, including the XKlp2 target protein (TPX2) and the important regulator Aurka, affect localization and activity<sup>6,7</sup>. The most well-known members of the Aurka kinase family are

#### Correspondence: Mehran Ullah

Department of Health, Medical Teaching Institution Mardan Medical Complex Mardan, KP, Pakistan  
Email: mehranullah1111@gmail.com  
Cell: +92-333-9852724

**Date Received:** May-14-2022

**Date Accepted:** June -22-2022

**Citations :** Muhammad Shahab, Mehran Ullah, Haider Ali Khan, Mehreen Ghufuran, Mohtasim Billah, & Muhammad Siddiq. (2022). ALLOSTERIC MODULATION OF AURKA KINASE ACTIVITY BY ARKIN-A VIA DYNAMIC CORRELATION NETWORK ANALYSIS: Original Article. Journal of Bacha Khan Medical College, 3(01), Page No. 45–57.  
<https://doi.org/10.69830/jbkmc.v3i01.29>

“Aurora A,” “(Aurora) B,” and “Aurora C,” which have sequences similar to those of yeasts and *Drosophila*. This family has not changed across evolution<sup>3</sup>. The carboxyl-terminal of human Aurka kinase enzymes has a highly conserved catalytic kinase domain. However, considerable sequence variability exists inside this area and plays a role in spatiotemporal localization. Several different cellular processes are caused by the presence of a kinase during the cell cycle<sup>8</sup>.

Specifically, Aurka Kinase is involved in the structure and operation of bipolar spindles, as well as centrosomal maturation and multiplication<sup>9, 10</sup>. Kinases are localized to a particular structure throughout the cell cycle, and during the interphase of cell division, there is a significant cytoplasmic pool of Aurka<sup>11, 12</sup>. Among the binding partners with which Aurora kinase interacts are Ajuba<sup>13</sup>, Arpc1b<sup>14</sup>, calmodulin<sup>15</sup>, CEP192<sup>16</sup>, NEDD9<sup>17</sup>, and Nucleophosmin B23<sup>18</sup>. The catalytic domain of the enzyme Aurka kinase has two lobes, much like threonine and serine kinase. Ectopic production of Aurka is carcinogenic because it causes tumors in animals and colonies to grow in cell culture<sup>19</sup>. Many strong Aurka kinase inhibitors are now being studied in humans after it was shown that they slowed the development of tumors in xenograft models.

Developing small molecular inhibitors using certain in-vitro and in-vivo techniques takes a lot of time and money. This kind of study also requires a higher degree of chemical synthesis competency, which must be assured to deliver a typical molecule. For this objective, molecular analyses were performed on the allosteric mechanism and dynamics in the complex structure of Aurka kinase and Tpx2 regulator and the allosteric inhibitory agent of AurkinA, a drug-like molecule.

## **MATERIALS AND PROCEDURES**

The 3D structures of 1OL5 (2.5 resolution) and 5DT4 (2.86 resolution) were obtained using the Protein Data Bank (PDB). SWISS-MODEL (expasy.org) was used to construct the missing residues of both proteins, 1OL5 (23–29, chain B) and 5DT4 (284–289), using the self-template approach. It was discovered that 5DT4 was bound to two co-crystal ligands: the allosteric ligand 5DN and the initial substrate ATP. There were no more magnesium ions in the system. However, a 43-amino-acid long peptide (Chain B) was inserted in the case of 1OL5. When

ADP was eliminated, both tyrosine residues (Tyr287, 288) remained phosphorylated. Principal Component Analysis (PCA)

Principal component analysis (PCA) detected substantial protein amplitude changes<sup>20</sup>. The cpptraj software created the covariance matrix using just C coordinates. The eigenvectors and eigenvalues were found by diagonalizing the covariance matrix. Eigenvalues reveal mean square fluctuation, whereas eigenvectors represent motion direction. Charting monitored PC1 and PC2, the first two key components.

Calculating Gibbs free energy. The equation for calculating binding energies,  $G_{\text{binding}}$ , is  $G_{\text{b}} = G_{\text{r}} + I - (G_{\text{r}} - G_{\text{l}}) \dots (a)$ <sup>21</sup>.

The total energy for substrate and effector Aurka-TPX2 and AurkinA-AurkinA is (G.R. and G.L.). M.D. simulation and free energy calculation can quantify binding energy in (MM/GBSA) molecular mechanics, generalized born surface area (MM/PBSA), and Poisson Boltzmann surface area for each individual's free energy as per equation (2).  $G$  equals  $(G_{\text{sa}} - TSS) + E_{\text{bonded}} + E_{\text{vd}} + E_{\text{e}} + G_{\text{pb}}$ . (2).

The solvated nonpolar and polar contribution energy is  $G(\text{S.A.}) - TSS$ , the electrostatic energy is  $E_{\text{e}}$ , the bonding free energy is  $E_{\text{bonded}}$ , the Vander Waals energy is  $E_{\text{vd}}$ , and so on. The solute entropy is ( $S_{\text{s}}$ ), while the absolute temperature is ( $T$ ).

## **RESULTS AND DISCUSSION**

AurkinA binds to Aurka hydrophobic pocket. The chemical mechanism by which AurkinA binding blocked the Aurka-TPX2 complex was revealed by the crystal structures of the Aurka kinase catalytic domain in isolation and liganded to AurkinA. AurkinA soaking in  $\text{Mg}^{2+}$ -ATP-AURKA crystals formed a 2.86-resolution liganded network (5DT4). Pymol displayed active and allosteric site regions. AurkinA was securely positioned into the pocket, and its orientation and placement were verified by a distinct signal originating from the bromine atom at the Meta position on the benzene ring (Figure 1). The N-lobes of the  $\alpha\text{C}$  and  $\alpha\text{B}$  helices created a hydrophobic channel where AurkinA was discovered (Figure 1a). The TPX2 YSY motif, which is essential for the Aurka-TPX2 interaction, is accommodated in this pocket in contrast to the structure of Aurka in conjunction with TPX2 (Figure 1b)<sup>22</sup>. The

hydrophobic pocket produced by L178, V182, H201, K166, E175, and E170 interacted with the quinoline and phenyl motifs of AurkinA, indicating the formation of hydrophobic contacts. An ionic connection was also established by the carboxylic acid of AurkinA and the basic side chain of K166. It became clear that the hydrophobic pocket that boosts the hydrophobicity of the pocket floor at the Meta position of the benzene ring was important.

The stability of the two systems was monitored by comparing the RMSD and RMSF of each snapshot to the original structure. All systems' C-alpha RMSD values were within 0.4 throughout the simulation. A 100ns M.D. simulation (with and without AurkinA medication) examined the intrinsic structure of Aurka. The stability of the Aurka-TPX2 and AurkinA systems and the backbone side chain's equilibration and deviation were assessed using the root mean square deviation (RMSD) (Figure 2). Lower deviation curves indicate more stable protein ensembles and vice versa. Comparing the bound and free Aurka systems' RMSD graphs to the original structure shows that 100ns is adequate to reach equilibrium at 310K. The RMSD of the Aurka-TPX2 system remains stable throughout the simulation in the absence of AurkinA drug (1OL5) because the Aurka pocket is bigger and has a better affinity for binding with the drug. It initially deviates from 0.2nm to 0.4 at 100ns M.D. simulation period. The Aurka-AurkinA (5DT4) system shows a higher RMSD value throughout the simulation, especially between 35 and 40 ns.

The Aurka-TPX2 system has a different backbone variation than the Aurka-AurkinA system. The Aurka-TPX2 RMSD graph showed a significant and quick shift in backbone deviation at 30ns from

0.17 ± 0.03 simulation period. RMSD increased and decreased somewhat. The RMSD is low in the absence of AurkinA (1OL5) and greater in its

presence (5DT4), demonstrating that AurkinA residues fluctuate and migrate strongly towards surrounding active site residues. Destabilization of AURKA caused a large 5DT4 backbone RMSD swing. Destabilization orders reduce TPX2 binding to active site residues even more, suggesting a distal impact on hydrogen bond contact or strength with the peptide, guaranteeing resistance to this phenomenon. Due to indirect de-stability, an allosteric action disrupts the Aurka-TPX2 binding site, preventing TPX2 from binding. Figure 2: Aurka-TPX2 and Aurka-AurkinA Root Mean Square Deviation (RMSD).

We examined the C-alpha root mean square fluctuation (RMSF) in the 1OL5 and 5DTN systems to understand better how amino acids and changes affect side-chain atom dynamics. The main chain root mean variation was calculated over the trajectories and averaged across each residue for Aurka-TPX2 (1OL5) and AurkinA (5DT4). The molecular dynamics simulation showed the most amino acid change in 140-145, 165-175, and 195-205. The simulation showed small 210-280 variations (Figure 3). This spectrum of amino acids has a higher allosteric effect on AurkinA inhibitor binding and TPX2 disruption. In the Aurka-TPX2 system, the RMSF shows slight fluctuation passion in particular residues compared to the AurkinA system. However, when the distal loop's distal position changes, the allosteric site residues vary more, suggesting that the Aurka-TPX2 TPX2 binding residues become more mobile, disrupting neighboring residues and making them resistant to AurkinA binding. Without the AurkinA medication, the AURKA showed minimal variation in passion in specific locations. Still, in the presence of the drug, it showed a strong pattern of

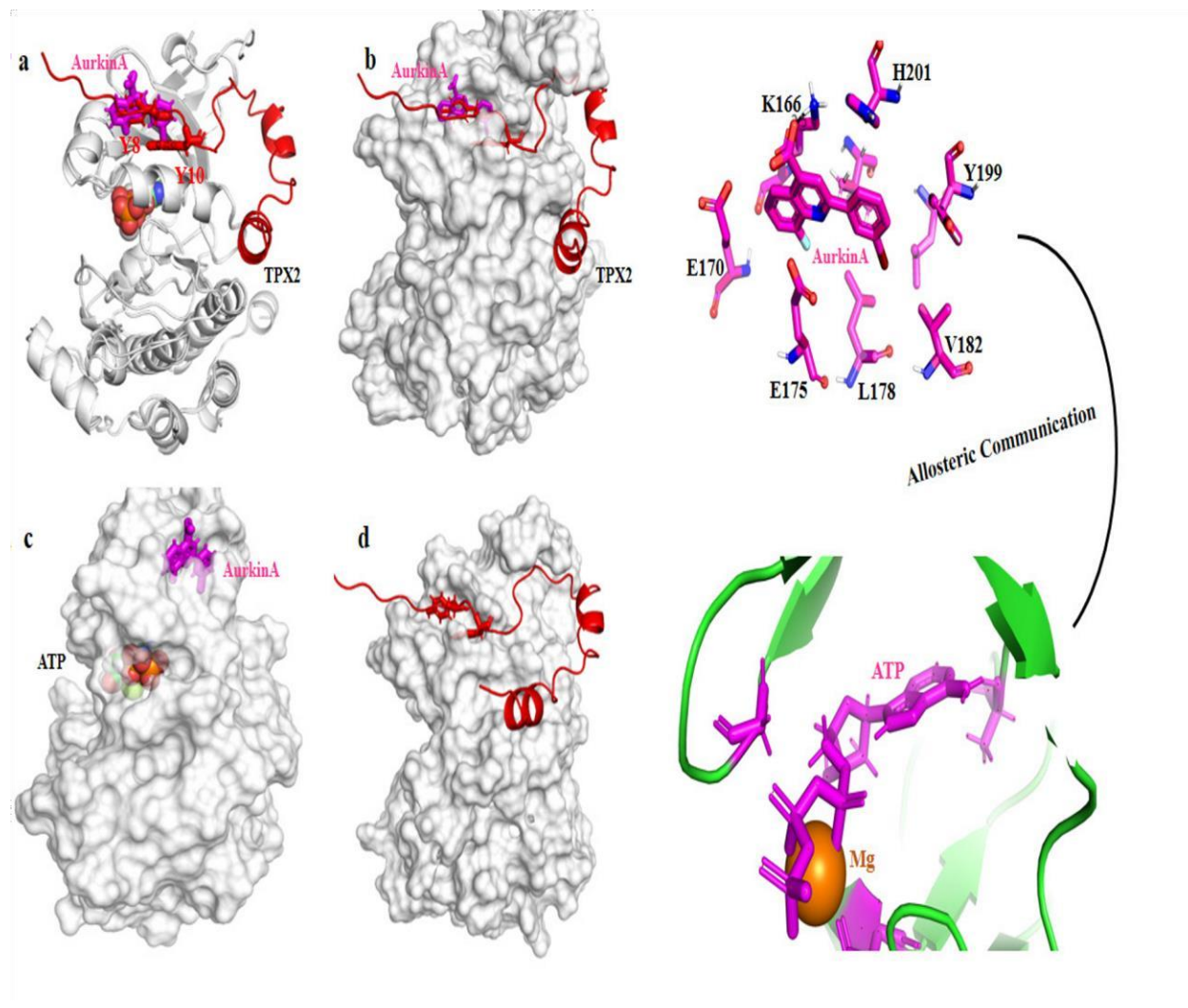
changes in the needed residues from 140 to 145. The binding of a small medication-like molecule destabi-

**Table 1: The MMPBSA Binding free energy (kcal/mol) calculation for Aurka-TPX2 complex.**

No	VDWAALS	EEL	EGB	ESURF	DELTA TOTAL BINDING FREE ENERGIES
1	-47.0269	-441.5410	454.9806	-6.6285	-41.3158

**Table 2: The MMPBSA Binding free energy (kcal/mol) calculation for Aurka-AurkinA complex**

No	VDWAALS	EEL	EPB	ENPOLAR	DELTA TOTAL BINDING FREE ENERGIES
----	---------	-----	-----	---------	-----------------------------------



1	-51.0269	-441.5410	458.4398	-37.7257	-6.9534
---	----------	-----------	----------	----------	---------

Figure 1: Binding of AurkinA causes conformational changes in the Aurka protein (a, b, c, d). Aurka kinase (126-390) crystal structure containing Mg<sup>+</sup>, ATP, and AurkinA (5DT4) coupled to it, aligned with TPX2 1-43. (1OL5, red). AurkinA (magentas) binds to the Y-S-Y motif of TPX2 binding pocket formed by the C and B helices. Above the ATP site is the hydrophobic Y-pocket location. AurkinA (magentas) and TPX2 from 8-11 bind to the Y-pocket in detail. (e) AurkinA binding position in the Y-pocket. AurkinA carboxylic acid interacts with K166 amine, which is stabilized by H201.

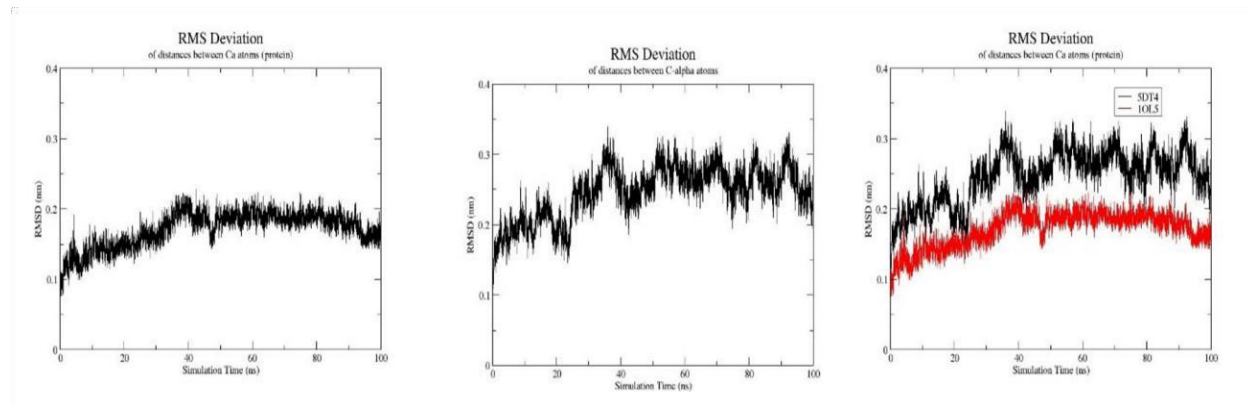


Figure 2: Aurka-TPX2 and Aurka-AurkinA Root Mean Square Deviation (RMSD).

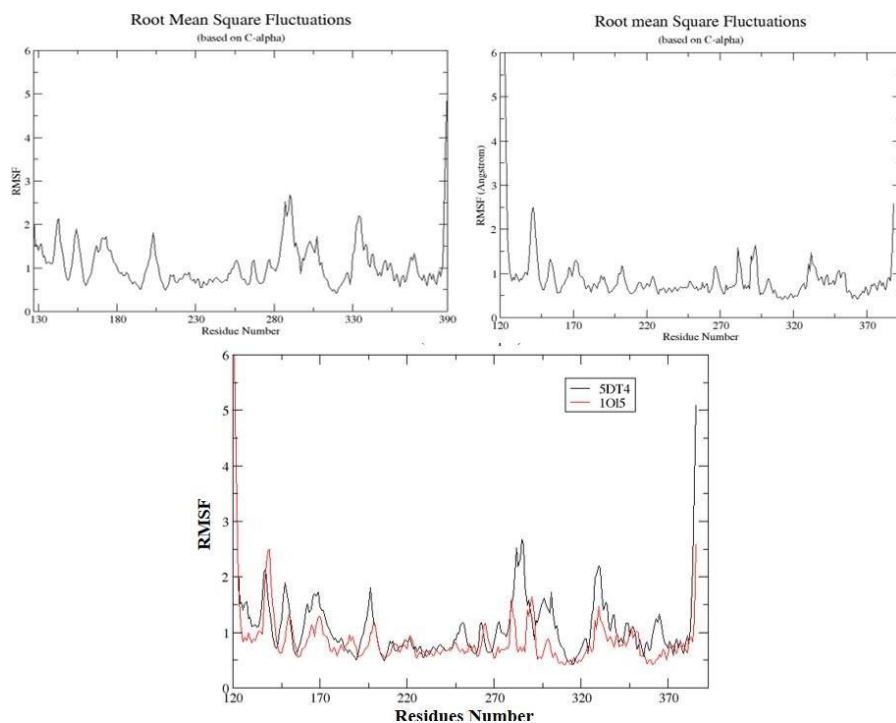


Figure 3: Aurka-TPX2 and Aurka-AurkinA Root Mean Square Deviation (RMSf).

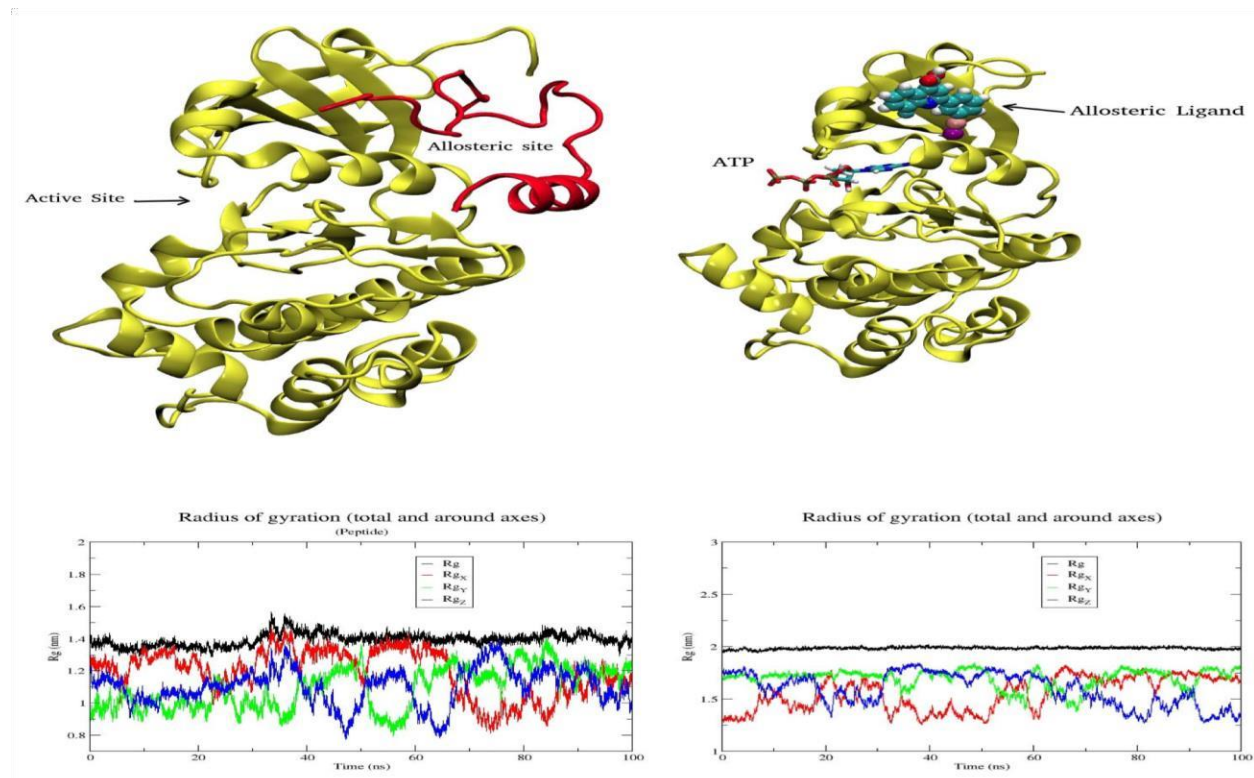
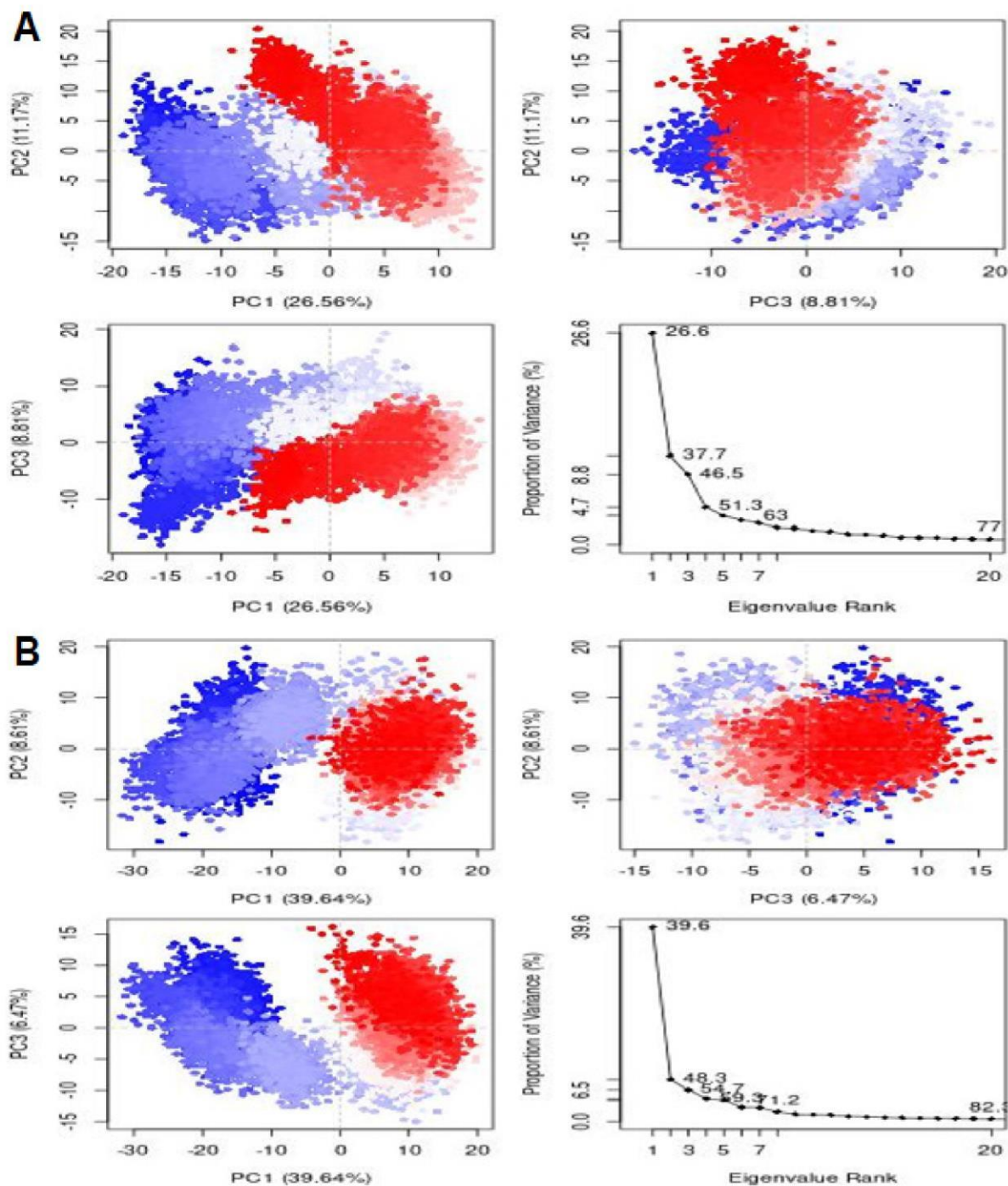


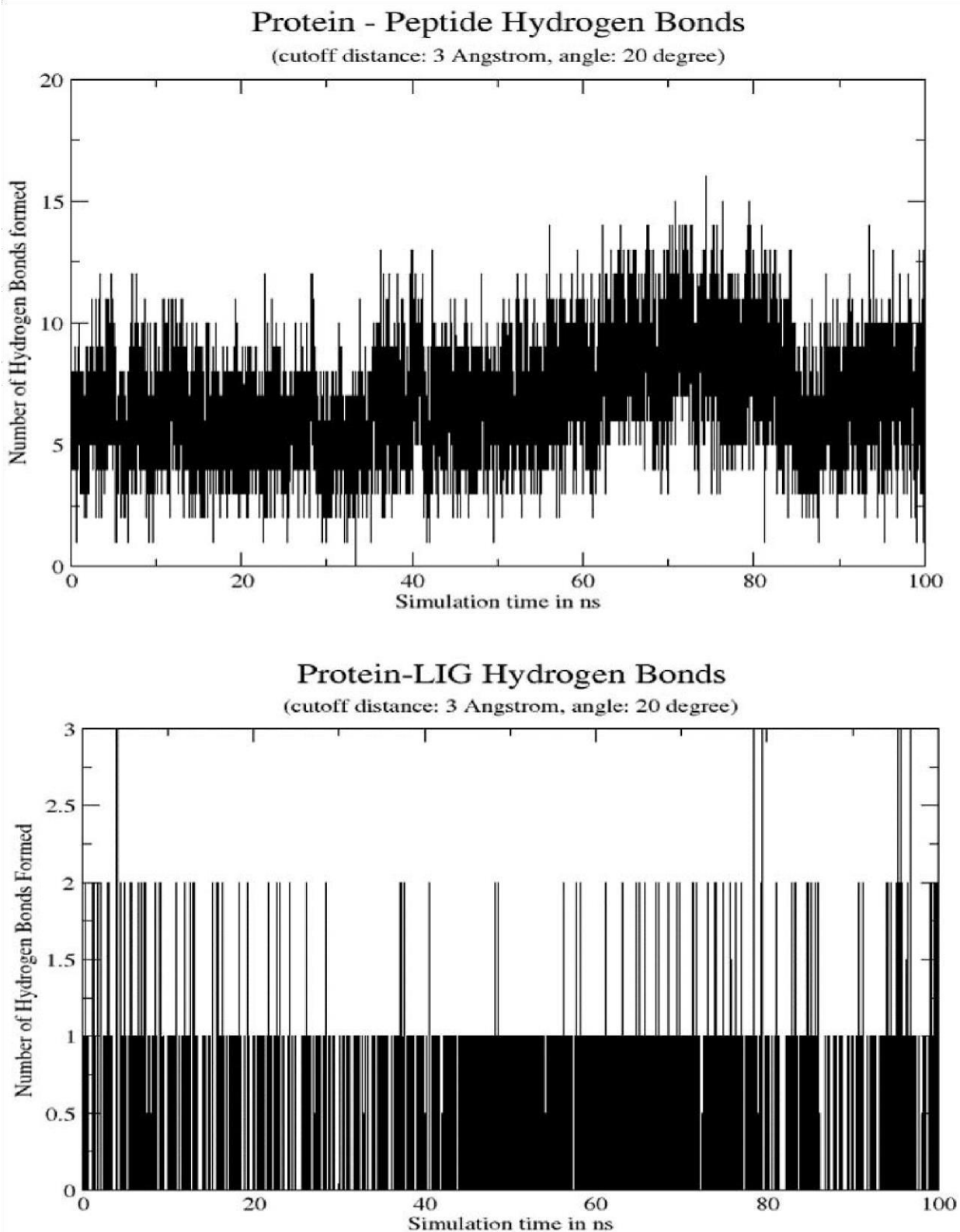
Figure 4: The average radius of gyration (RoG) for peptide coupled to protein based on the Ca atom is 1.39



0.04 nm. Between 30 and 40 ns, there is a notable difference. Because the peptide is a tiny molecule, it exhibits significantly larger fluctuations than the protein, as seen by RMSd, RMSf, and RoG. During the simulation, the peptide stayed compact in general.

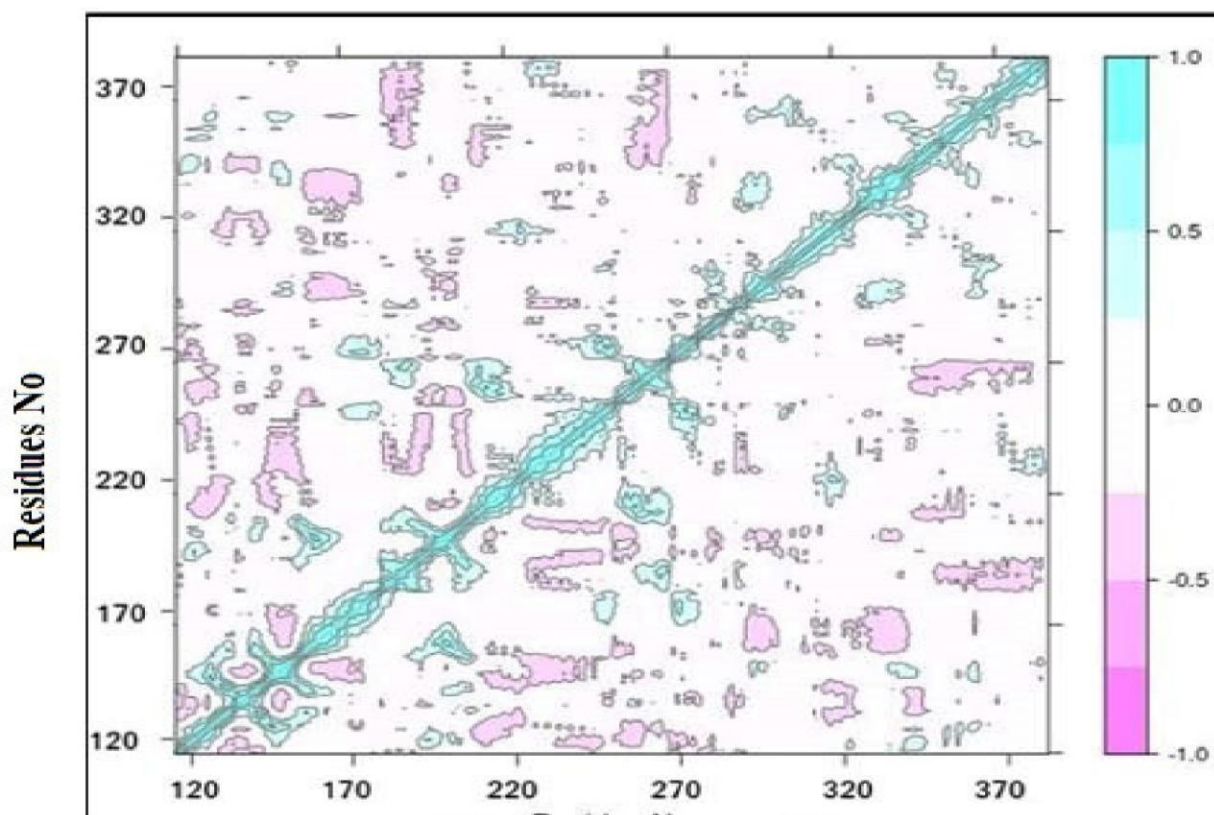
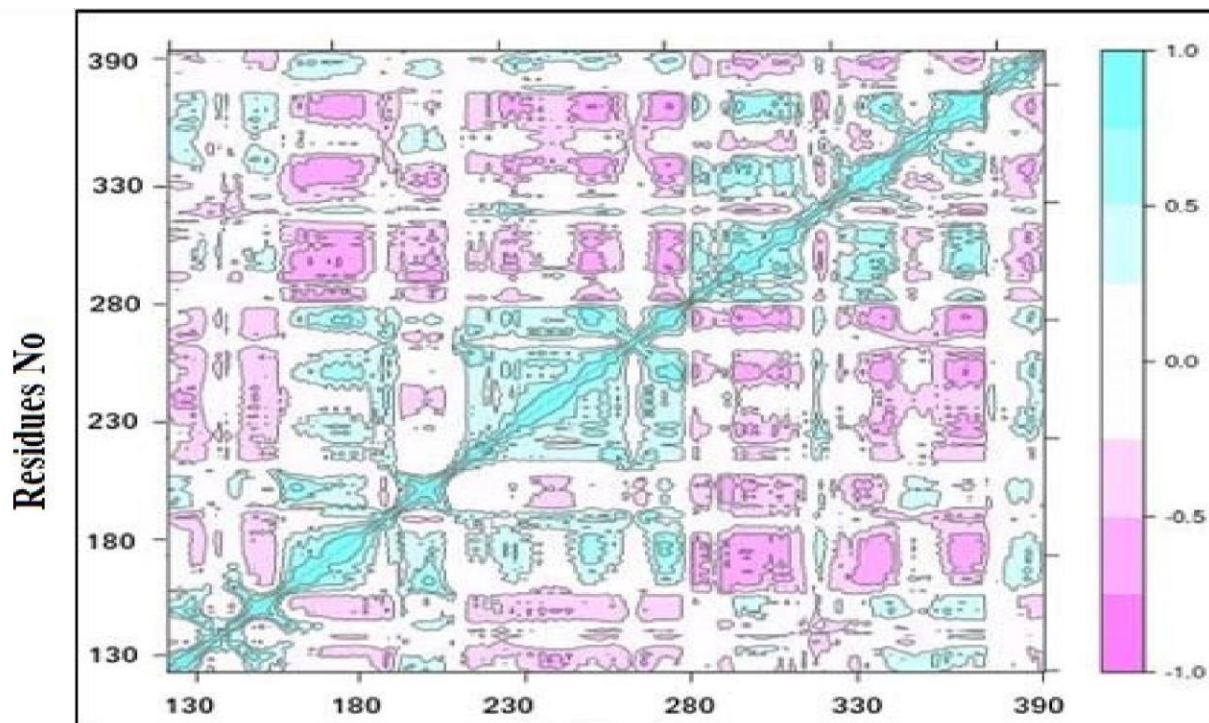
Figure 5: Principle Component Analysis (PCA) with the R software. The first three main components account for 46.5 percent of the total coverage. (B) Using the R tool to perform Principle Component Analysis (PCA). The coverage of the first three main components is 54.7 percent.

Figure 6: During a 100ns simulation, the total number of hydrogen bonds created between a protein and a peptide molecule, as well as the total number of hydrogen bonds formed between a protein and a 5DN (



allosteric ligand) molecule.

Figure 7: Matrix plot for protein residues using Dynamic Cross Correlation (DCCM). Positive connection is shown by the blue color. The pink color indicates a bad relationship. There is no association between protein



**Residues No**

residues when the color white.

lized AurkA-TPX2, halting enzyme activity throughout the cell cycle, suggesting an allosteric mechanism and active site pocket closure and opening.

**Folding Dynamics (Gyration Radius).** The radius of gyration and solvent-accessible surface area analysis indicated 5DTN and 1OL5 compactness. The radius of gyration is the mass-weighted root mean square distance of atom clusters from their center of mass. A key protein size indicator is the radius of gyration (RoG). Figure 4 shows the C-alpha atom's Radius of Gyration (RoG) for 1OL5 and 5DT4 after 100ns of simulation at 300K. AurkA-TPX2 and AurkA-AurkinA's RoG were calculated. Based on the Ca atom, a peptide linked to a protein has an average RoG of 1.39 0.04 nm. A change is seen between 30 and 40 ns. Protein-coupled to inhibitors with Ca atoms has a typical Radius of Gyration (RoG) of 1.94 0.02. Protein compactness hardly changed. The time-dependent RoG measures compactness and folding. A misfolded protein's RoG changes with time, whereas a stably folded protein's does not. Consistent RoG values imply protein folding stability, whereas deviations indicate folding instability<sup>23</sup>. AurkinA connected to protein is more stable than TPX2 bound to inhibitor, meaning proper simulated folding. Alterations distant from the active site may affect the binding pocket significantly. These locations may effectively communicate enzyme function in signal transmission during biological activity.

**Principal Component Analysis PCA analysis** was done on all systems throughout the 100ns simulation to identify the rigorous motion of the AurkAA-TPX2 and AurkA-AurkinA structures. Snapshots are taken every two seconds. In major component analysis, all three facilities show distinct conformational changes, clockwise and anti-clockwise. PCA analysis shows active site residue mobility. The enzyme's free form undergoes conformational modifications such as anti-clockwise thumb domain rotation along the core helix axis, finger domain motion, and amino-terminal and COOH terminal linker movement. Mobility indicates enzyme stability during polymerization (Figure 5).

**Hydrogen bonds Analysis.** Hydrogen bonding is essential for protein structural stability and molecular recognition. The AurkA-TPX2 and AurkinA-AurkinA/LIG structures' intermolecular hydrogen bonds were examined during the 100ns M.D. simulation phase. AurkA-TPX2 has more hydrogen bonds than AurkA-AurkinA/LIG. AURKA-TPX2

has some flexibility since there are fewer hydrogen bonds to form. Over time, the greater number of hydrogen bonds in AURKA-TPX2 affects its disruption and binding to LIG (Figure 6).

**Dynamic Cross Co-Relations Map (DCCM).**

The degree of cross co-relation between the various residues in the Aurka complex has supplied important information about the allosteric and catalytic sites. As a result, a dynamic cross-correlation map (DCCM) for free Aurka and Aurka/AurkinA systems was constructed using the cross-correlation coefficient from molecular dynamics trajectories.

A positive and negative correlation is shown by the top and bottom triangles of the DCCM, respectively. Observing the diagonal allows us to notice the classic cross-correlation in the helices. The DCCM analysis (Figure 7) clarifies the passage of allosteric signals from the allosteric site to the catalytic site in the 5DT4 bound state, which includes dynamical communication information in the domain of these residues.

## **CONCLUSION**

The research uses cross-correlation network analysis and molecular dynamics simulation to describe the allosteric mechanism of Aurka kinase for AurkinA. In the presence of AurkinA, the Aurka kinase displayed a greater pattern of fluctuation in active site regions such as L178, V182, H201, K166, E175, and E170, indicating the narrowing of the gorge bottleneck, which inhibited substrate access in the active side. In the absence of AurkinA, the enzyme displayed a slightly low fluctuation passion in some regions. Inbound structure, AURKA/AurkinA has a greater RMSD value than AurkA-TPX2, indicating that residues near the active site with a higher RMSD value also have a higher RMSD value. Then, A dynamic cross-correlation map in the Aurka/AurkinA and free systems reveals catalytic-allosteric site interactions. The DCCM analysis found that dynamical communication information in the domain of these residues at the allosteric site transmits allosteric signals to the catalytic site in the Aurka-bound state.

Further research reveals that AurkinA binding affects Tpx2 binding and allosteric effects on the approximately placed active site residues, showing that shutting and opening patterns affect the functional site pocket. These variants impair TPX2 binding, making 5DT4 TPX2-resistant. This detailed

study will show how allosteric inhibitors restrict Aurka kinase activity and complex structure conformation.

## REFERENCES

1. Bischoff, J.R., et al., A homolog of *Drosophila aurora* kinase is oncogenic and amplified in human colorectal cancers. *The EMBO journal*, 1998. 17(11): p. 3052-3065.
2. Goldenson, B. and J.D. Crispino, The aurora kinases in cell cycle and leukemia. *Oncogene*, 2015. 34(5): p. 537545.
3. Geschwindner, S., J. Ulander, and P. Johansson, Ligand binding thermodynamics in drug discovery: still a hot tip? *Journal of Medicinal Chemistry*, 2015. 58(16): p. 6321-6335.
4. Gautschi, O. et al., Aurora kinases as anticancer drug targets. *Clinical Cancer Research*, 2008. 14(6): p. 16391648.
5. Nikonova, A.S., et al., Aurora A kinase (AURKA) in normal and pathological cell division. *Cellular and Molecular Life Sciences*, 2013. 70(4): p. 661-687.
6. Zhao, B., et al., Modulation of kinase-inhibitor interactions by auxiliary protein binding: Crystallography studies on Aurora A interactions with VX-680 and TPX2. *Protein Science*, 2008. 17(10): p. 1791-1797.
7. Eyers, P.A. and J.L. Maller, Regulation of *Xenopus* Aurora A activation by TPX2. *Journal of Biological Chemistry*, 2004. 279(10): p. 9008-9015.
8. Carlton, J.G., H. Jones, and U.S. Eggert, Membrane and organelle dynamics during cell division. *Nature Reviews Molecular Cell Biology*, 2020. 21(3): p. 151-166.
9. Dodson, C.A. and R. Bayliss, Activation of Aurora-A kinase by protein partner binding and phosphorylation are independent and synergistic. *Journal of Biological Chemistry*, 2012. 287(2): p. 1150-1157.
10. Fabbro, D. et al., Abl kinase inhibitors directed at the ATP or myristate-binding site. *Biochimica et Biophysica Acta (BBA)-Proteins and Proteomics*, 2010. 1804(3): p. 454-462.
11. Bayliss, R., et al., On the molecular mechanisms of mitotic kinase activation. *Open biology*, 2012. 2(11): p. 120136.
12. Zorba, A., et al., Molecular mechanism of Aurora A kinase autophosphorylation and its allosteric activation by TPX2. *Elife*, 2014. 3: p. e02667.
13. Schimizzi, G.V. and G.D. Longmore, Ajuba proteins. *Current Biology*, 2015. 25(11): p. R445-R446.
14. Molli, P.R. et al., Arpc1b, a centrosomal protein, is an activator and substrate of Aurora A. *Journal of Cell Biology*, 2010. 190(1): p. 101-114.
15. Klee, C.B. and T.C. Vanaman, Calmodulin. *Advances in protein chemistry*, 1982. 35: p. 213-321.
16. Gomez-Ferreria, M.A. et al., Human Cep192 is required for mitotic centrosome and spindle assembly. *Current Biology*, 2007. 17(22): p. 1960-1966.
17. Pugacheva, E.N. and E.A. Golemis, The focal adhesion scaffolding protein HEF1 regulates activation of the Aurora-A and Nek2 kinases at the centrosome. *Nature Cell Biology*, 2005. 7(10): p. 937-946.
- 18.

Reboutier, D. et al., Nucleophosmin/B23 activates Aurora A at the centrosome through serine phosphorylation 89. *Journal of Cell Biology*, 2012. 197(1): p. 19-26.

19. Scott, D.E., et al., Using a fragment-based approach to target protein-protein interactions. *ChemBioChem*, 2013. 14(3): p. 332.
20. Balsera, M.A., et al., Principal component analysis and long time protein dynamics. *The Journal of Physical Chemistry*, 1996. 100(7): p. 2567-2572.
21. Massova, I. and P.A. Kollman, Combined molecular mechanical and continuum solvent approach (MM-PBSA/GBSA) to predict ligand binding. *Perspectives in drug discovery and design*, 2000. 18(1): p. 113-135.
22. Bird, A.W. and A.A. Hyman, Building a spindle of the correct length in human cells requires the interaction between TPX2 and Aurora A. *The Journal of Cell Biology*, 2008. 182(2): p. 289-300.

**Disclaimer:** Nil

**Conflict of Interest:** There is no conflict of interest.

**Funding Disclosure:** Nil

**Authors Contribution**

**Concept & Design of Study:** Muhammad Shahab1

**Data Analysis:** Mehran Ullah\*2, Haider Ali Khan, Muhammad Siddiq6

**Critical Review:** Mehreen Ghufra5, Mohtasim Billah5

**Final Approval of version:** Muhammad Shahab1



**Open Access:** This article is licensed under a Creative Commons Attribution 4.0 International License, which permits use, sharing, adaptation, distribution and reproduction in any medium or format, as long as you give appropriate credit to the original author(s) and the source, provide a link to the Creative Commons license, and indicate if changes were made. The images or other third party material in this article are included in the article's Creative Commons license, unless indicated otherwise in a credit line to the material. If material is not included in the article's Creative Commons license and your intended use is not permitted by statutory regulation or exceeds the permitted use, you will need to obtain permission directly from the copyright holder. To view a copy of this license, visit <http://creativecommons.org/licenses/by/4.0/>. © The Author(s) 2022